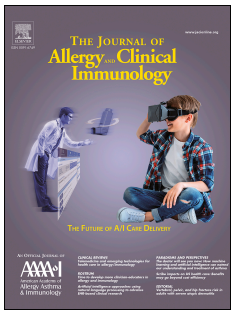
Journal Pre-proof



Real-time imaging of asthmatic epithelial cells identifies migratory deficiencies under Type-2 conditions

Mingzhu Jin, MD, Simon Watkins, PhD, Yolanda Larriba, PhD, Callen Wallace, PhD, Claudette St. Croix, PhD, Xiuxia Zhou, PhD, Jinming Zhao, PhD, Shyamal Peddada, PhD, Sally E. Wenzel, MD

PII: S0091-6749(21)01402-0

DOI: https://doi.org/10.1016/j.jaci.2021.08.027

Reference: YMAI 15275

To appear in: *Journal of Allergy and Clinical Immunology*

Received Date: 22 June 2021

Revised Date: 5 August 2021

Accepted Date: 27 August 2021

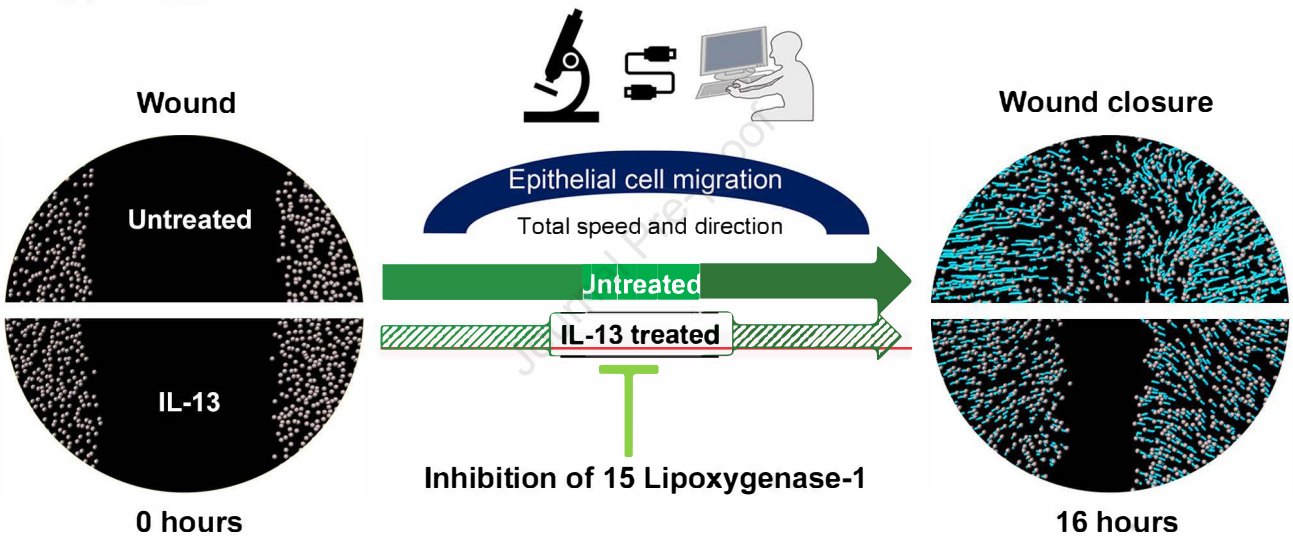
Please cite this article as: Jin M, Watkins S, Larriba Y, Wallace C, St. Croix C, Zhou X, Zhao J, Peddada S, Wenzel SE, Real-time imaging of asthmatic epithelial cells identifies migratory deficiencies under Type-2 conditions, *Journal of Allergy and Clinical Immunology* (2021), doi: https://doi.org/10.1016/j.jaci.2021.08.027.

This is a PDF file of an article that has undergone enhancements after acceptance, such as the addition of a cover page and metadata, and formatting for readability, but it is not yet the definitive version of record. This version will undergo additional copyediting, typesetting and review before it is published in its final form, but we are providing this version to give early visibility of the article. Please note that, during the production process, errors may be discovered which could affect the content, and all legal disclaimers that apply to the journal pertain.

© 2021 Published by Elsevier Inc. on behalf of the American Academy of Allergy, Asthma & Immunology.

Journal Pre-proof

Real-time imaging of asthmatic epithelial cells identifies migratory deficiencies under Type-2 conditions



Human airway epithelial cells
from 12 mild-moderate asthma patients

IL-13 alters cell migration
to limit wound closure

Journal Pre-proof

Real-time imaging of asthmatic epithelial cells identifies migratory deficiencies under Type-2 conditions

Mingzhu Jin, MD[1,2], Simon Watkins, PhD[3], Yolanda Larriba, PhD[4], Callen Wallace, PhD[3], Claudette St. Croix, PhD[3], Xiuxia Zhou, PhD[1], Jinming Zhao, PhD[1], Shyamal Peddada, PhD[5], Sally E. Wenzel*, MD[1,6]

1. Department of Environmental and Occupational Health, Graduate School of Public Health, University of Pittsburgh, Pittsburgh, USA
2. Department of Rhinology, Shengjing Hospital of China Medical University, Shenyang, China
3. Center for Biologic Imaging, School of Medicine, University of Pittsburgh, Pittsburgh, USA
4. Department of Statistics and Operations Research, Universidad de Valladolid, Valladolid, Spain
5. Department of Biostatistics, Graduate School of Public Health, University of Pittsburgh, Pittsburgh, USA
6. Asthma and Environmental Lung Health Institute @UPMC, Pittsburgh, USA

Corresponding Author:

Sally E. Wenzel, MD
4127 Public Health
130 Desoto Street
Pittsburgh, PA. 15261
swenzel@pitt.edu
412-647-9345

Journal Pre-proof

Conflicts of Interest:

Mingzhu Jin, MD: No conflicts of interest

Simon Watkins, PhD: No conflicts of interest

Yolanda Larriba, PhD: No Conflicts of Interest

Callen Wallace, PhD: No Conflicts of Interest

Claudette St. Croix, PhD: No Conflicts of Interest

Xiuxia Zhou, PhD: No Conflicts of Interest

Jinming Zhao, PhD: No Conflicts of Interest

Shyamal Peddada, PhD: No Conflicts of Interest

Sally E. Wenzel*, MD: No Conflicts of Interest directly related to this manuscript. Dr. Wenzel declares additional unrelated conflicts of interest related to consulting with Sanofi (dupilumab), AstraZeneca (Tezepelumab), GSK (mepolizumab), Knopp (dexpramipexole) and multicenter research grants with AstraZeneca (Tezepelumab and Benralizumab), GSK (anti-IL33), Knopp Bioscience (dexpramipexole). She has also received unrestricted research support for the Severe Asthma Research Program (unrelated to this study) from TEVA and Boehringer Ingelheim. She received institutional research support from Pieris.

Journal Pre-proof

Abstract

Background: The epithelium is increasingly recognized as a pathologic contributor to asthma and its phenotypes. Although delayed wound closure by asthmatic epithelial cells is consistently observed, underlying mechanisms remain poorly understood, partly due to difficulties in studying dynamic physiologic processes involving polarized multilayered cell systems. Although Type-2 immunity has been suggested to play a role, the mechanisms by which repair is diminished are unclear.

Objective: To develop and utilize primary multilayered polarized epithelial cell systems, derived from asthmatic patients, to evaluate cell migration in response to wounding under Type-2 and untreated conditions.

Methods: A novel wounding device for multilayered polarized cells, along with time-lapse live cell/real-time confocal imaging were evaluated under IL-13 and untreated conditions. The influence of inhibition of the Type-2 enzyme, 15 lipoxygenase (15LO1), on the process was also addressed. Cell migration patterns were analyzed by high dimensional Frequency Modulated Möbius for statistical comparisons.

Results: IL-13 stimulation negatively impacts wound healing by altering the Total speed, directionality and acceleration of individual cells. Inhibition 15LO1 partially improved the wound repair through improving Total speed.

Conclusions: Migration abnormalities contributed to markedly slower wound closure of IL-13 treated cells, which was modestly reversed by 15LO1 inhibition, suggesting its potential as an asthma therapeutic target. These novel methodologies offer new ways to dynamically study cell movements and identify contributing pathologic processes.

Key Messages

IL-13 decreases AECs wound repair by delaying migration patterns. 15LO1 inhibition partially recovers the delayed wound repair.

Capsule summary

Using cutting-edge real-time confocal technology and advanced statistical methods, this article

identified marked abnormalities in the wound repair and migratory patterns of asthmatic airway epithelial cells (AECs) under Type-2/IL-13 immune conditions.

Keywords: asthma; airway epithelial cells; wound repair; cell migration; IL-13, Type-2

Abbreviations:

AECs: Airway epithelial cells

ALI: Air Liquid Interface

AUC: Area under the curve

BH procedure: Benjamini & Hochberg procedure

DMSO: Dimethyl sulfoxide

FeNO: Fraction exhaled NO

FMM model: Frequency Modulated Möbius model

15LO1: 15 lipoxygenase 1

15 HpETE: 15 hydroperoxyeicosaetetranoic acid

MMA: Mild-Moderate asthmatic

T2: Type 2

PE: phosphatidylethanolamine

PI3K: phosphatidyl inositol 3 kinase

Journal Pre-proof

Introduction

Asthma is a chronic respiratory disease, affecting more than 300 million people worldwide[1]. Epithelial dysfunction is increasingly recognized as relevant to its pathogenesis, with underlying genetic and genomic epithelial abnormalities contributing to the consistent observations of delayed wound closure by asthmatic airway epithelial cells (AECs)[2–6]. Maintaining an intact epithelial barrier in the face of injury requires at least 2 processes: 1) initial migration, 2) later proliferation. Slower migration and more random movement was observed in poorly differentiated/submerged AECs from asthmatic/wheezy children[2,7]. A role for Type-2 (T2) inflammation in this dysregulation has been suggested, with a recent study showing that IL-4/-13 treatment also delayed wound healing of undifferentiated AECs[8]. This finding is consistent with the slower wound closure observed in asthma patients with elevations in the T2/IL-13 biomarker, fraction exhaled NO (FeNO)[4].

IL-4 and -13 also induce high expression and activity of 15 lipoxygenase 1 (15LO1), an enzyme highly expressed in asthmatic AECs which contributes to mucus production and secretion[9–11]. 15LO1 is linked to cell death pathways, in particular ferroptosis[12] and compensatory induction of cell survival through mitophagy/autophagy, suggesting a cell phenotype struggling for survival[13]. Yet, its role in wound repair is unknown.

Studies of epithelial wounding in human model systems are challenging. Almost all studies are done in submerged monolayers of poorly differentiated cells which do not mirror the multilayered polarized human columnar airway epithelium. Air Liquid Interface (ALI) culture reasonably reflects these complex *in vivo* conditions[14], but these multilayered systems with tight cell-cell connections impact the ability to consistently perform precise wounds, even using novel circular wounding patterns[15–17]. Further, tracking and then interpretation of the complex multi-directional individual cell

movements in multi-layered systems is challenging.

Based on this background, we developed a novel *in vitro* wounding system applicable to highly differentiated primary human AECs. Using this system, we hypothesized that T2-inflammation, would reduce wound closure in asthmatic well differentiated, polarized AECs as compared to untreated cells. This delayed closure would be driven primarily by abnormally slow cell migration. We further hypothesized that inhibition of 15LO1 would improve the IL-13-driven poor wound closure. Our approach involved innovative approaches to measure and analyze single cell migration in multi-layered systems recorded in real-time under T2 and non-T2 (untreated) conditions.

Journal Pre-proof

Methods

Participants and Bronchoscopy

Participants were recruited as part of the Immune Mechanisms of Severe Asthma program (P01 AI106684). AECs were obtained by bronchoscopic brushing of Mild-Moderate asthmatic (MMA) subjects as previously described[18]. All 12 donor cell lines were maintained separately. The results reflect the data for 12 individual/distinct human donors. The study was approved by the Institutional Review Board of the University of Pittsburgh and all participants provided informed consent. For details, see the Methods section in the Online Repository.

ALI culture

AECs were cultured as previously described[11,19]. For details, see the Methods section in the Online Repository.

Wounding method

Traditional models of physical wounding of AECs using pipette tips or other devices often form irregular shaped wounds, particularly in the less stable transwell membrane system. We designed a novel device (see Fig. E1 in the Online Repository) specific for ALI cultured AECs. For details, see the Methods section in the Online Repository.

Measurement of Wound Repair

After wounding, the healing process was observed under live cell microscopy (Nikon A1), with the percentage remaining monitored using high resolution, large area (2×10mm) time-lapse imaging over a 48-hr period. Fixed images were taken every 8 hrs. After each 8 hr time point, cells were re-incubated in 5% CO2 at 37□. Percent of wound closure was calculated as: (the area of original wound - wound remaining)/original wound.

177

178 **Measurement of Migration**

179 Real-time live imaging of migration of primary cells in ALI was developed by Dr. Simon
180 Watkins, Center for Biological Imaging, University of Pittsburgh. We measured the
181 single cell migration by speed (Total speed), directionality (X-axis speed) and acceleration.

182

183 *Total speed*: Total distance of cells moved per unit time without accounting for direction.
184 The speed of the cells was represented as the average speed of all tracked AECs
185 (~1,000 cells) in a given condition.

186

187 *Acceleration*: Acceleration was measured by the formula (Total $speed_t$ -Total $speed_{t-3hrs}$) / (3 hrs)
188

189

190 *X-axis speed*: Unlike Total speed, this measurement accounted for only the distance
191 of movement towards the wound (X-axis) and measured as distance moved toward
192 the X-axis per unit time. When cells moved away from the wound (or opposite to the
193 wound center), a negative value was obtained. The total X-axis speed of the cells was
194 calculated by averaging X-axis speed of all tracked AECs.

195

196 For details, see the Methods section in the Online Repository.

197

198 **Western Blots**

199 AECs were cultured as previously described[11,19]. AECs at ALI day 7 were collected for
200 analysis of protein expression. For details, see the Methods section in the Online
201 Repository.

202

203 **Statistical Methods**

The comparison of area under the curve (AUC) for matched pair data (wound closure) between experimental groups was performed using standard paired t-tests of the AUCs and then by individual 8 hr time points. For cell migration experiments, we developed a parametric model to describe the temporal speed of motion of cells in each group using the Frequency Modulated Möbius (FMM)[20] model. Both Total speed as well as the X-axis speed were modeled using the FMM model. From the FMM model we derived five biologically relevant parameters for this study, namely, (i) intercept, the initial speed, (ii) amplitude or maximum speed from the initial speed, (iii) time to amplitude, (iv) skewness or how slowly the curve decays (close to zero would correspond to slowly decaying curve and close to -1 corresponds to a symmetric and quickly decaying curve), and (v) peakedness, which measures how sharp or blunted the peak is (the larger the value the sharper the peak). Description of skewness and peakedness is shown in Figure E2 in the Online Repository. Using the methodology developed in[20], we estimated the above parameters for each experimental group and constructed 95% confidence intervals for differences between experimental groups. If overall significance in these parameters was established, then paired analysis of each time point was performed, correcting for multiple comparisons using the Benjamini & Hochberg (BH) procedure. We used single parameter t-tests to test if acceleration is 0 $\mu m/hr^2$. As there were 8 time points, multiple testing was adjusted by BH procedure.

Journal Pre-proof

Results

IL-13 markedly impairs epithelial wound closure

AECs from 12 different MMA patients were utilized for all the wound repair studies in this report (See Table E1 in the Online Repository for patient characteristics). We previously reported that wound repair was delayed in asthmatic AECs compared to those from healthy participants particularly in those with elevated FeNO levels, a known biomarker of T2 inflammation[4]. To better understand the cellular processes and mechanisms behind the diminished wound repair, we developed an *in vitro* model utilizing IL-13 10 ng/ml stimulation (for 7 days) of ALI-cultured asthmatic AECs in a novel scratch wound model, which improved the consistency of the wounded area and depth (see Fig. E1 in the Online Repository)**.** IL-13 decreased the overall wound repair, as depicted by the differences in the AUC compared to untreated AECs, during the 48 hrs post wounding (Fig. 1 *A, B*) (n=6, p=0.028) (Fig. 1 *C*). We then compared individual 8 hr incremental time points (Fig. 1 *C*). At 8 and 16 hrs, the wound area under IL-13 conditions was greater than that under untreated conditions (n=6, p=0.017 for both). There were no differences at later time points (24, 32, 40 and 48 hrs). There were no differences in initial wound area under untreated or IL-13 conditions as shown in Figure E3 in the Online Repository.

IL-13 alters AEC migratory patterns following wounding as compared to untreated cells

To better identify cells and their movement in real-time, AEC nuclei were dyed with Hoechst 33324 (Fig. 2 *A, B*). Matching phase-contrast images of wound closure are shown in Figure E4 in the Online Repository. See Movie E2 in the Online Repository for dynamic imaging. Two parameters were identified to describe cell movement (see Fig. E5 in the Online Repository): Total speed (regardless of direction) and X-axis speed [as the net speed towards the wound center (directionality)].

Given the complex nature of these cell migration patterns, we applied the flexible FMM model[20] to characterize various parameters of speed, as described in Methods. Evaluating overall speed patterns, untreated cells displayed higher initial Total speed and had a later time to peak speed as compared to IL-13 treated cells, with significant differences in both by FMM parameters (Fig. 3 *A* and Table 1). As anticipated from the movies, X-axis (directional) speed patterns were substantially different between untreated and IL-13 treated cells (Fig. 3 *B* and Table 2). Although there were no differences in their initial X-axis speeds, untreated cells had almost twice the amplitude increase in X-axis speed compared to the IL-13 cells, indicative of a higher peak speed in the targeted X-axis direction in untreated. This greater X-axis amplitude was accompanied by a longer time to peak X-axis speed for the untreated cells, suggesting a more prolonged directed X-axis movement [8.95 hrs versus 7.06 hrs ($P < 0.05$)]. Furthermore, the FMM curve for the untreated cells decayed more rapidly than the IL-13 treated cells leading to significant differences in skewness between the two [-0.81 versus 0.09 ($P < 0.05$)] (Fig. 3 *C, D*). These differences exemplify the higher prolonged X-axis speed of untreated AECs at ~10 hrs (prior to wound closure), but not surprisingly, their near complete loss of directionality by 22 hrs once the wound closed. In contrast, IL-13 treated cells continued migrating slowly in the direction of the wound (X-axis) long after the untreated cells.

With confirmation of these overall differences by FMM, individual data points for Total (Fig. 3 *C*) and X-axis speed (Fig. 3 *D*) were then compared between IL-13 treated and untreated cells.

Speed: By paired testing, the initial Total Speed of the IL-13 treated cells (16.5±2.3 μm/h at 20 min) was slower than the untreated group (28.4±2.2 μm/h) ($p=0.043$).

Differences in Total speed persisted at 51 of the 72 (20 min) time points measured over the first 24 hrs and 72 of 72 timepoints from 24-48 hrs. All paired T-tests were corrected for multiple comparisons using BH correction (Fig. 3 *C* and Tables E2 and E3 in the Online Repository).

For X-axis speed, after BH correction, there were no differences in any of the 72 measurements between untreated and IL-13 treated cells over the first 24 hrs. However, during the second 24 hr period, 43 out the 72 time points had lower X-axis speed in the untreated compared to the IL-13 treated group (Fig. 3 *D* and Table E4 and E5 in the Online Repository).

Acceleration. We then tested if total acceleration was different from 0 $\mu m/h^2$, at individual incremental time points over 3 hr intervals (BH correction for multiple t-tests). Even with higher starting speeds, cells in the untreated group accelerate up to 9 hrs with an acceleration of 2.2 $\mu m/h^2$ ($p = 0.01$). As they approach the opposite wound edge, they cease to accelerate ($p > 0.05$). Interestingly, the IL-13 treated cells have a more rapid acceleration during the first 3 hrs with an estimated acceleration of 3.5 $\mu m/h^2$ ($p < 0.001$) but ceased to accelerate after only 6 hrs ($p > 0.05$) (Fig. 3 *E*).

Abnormal wound closure under IL-13 conditions is partially dependent on 15LO1 pathway activity

Consistent with previous studies[10], 15LO1 expression was markedly upregulated by IL-13 (Fig. 4 *A*). BLX2477 is a selective and specific 15LO1 inhibitor[19], which markedly inhibits formation of 15 hydroperoxyeicosaetetranoic acid (15 HpETE), which in IL-13 treated AECs is primarily conjugated with phosphatidylethanolamine (PE)[10,12]. Wound closure was compared between Dimethyl sulfoxide (DMSO) and BLX2477/DMSO under IL-13 conditions by AUC (Fig.4 *B, C*). BLX2477 increased the AUC compared to

DMSO (BLX 68.82% DMSO 62.27%, p=0.034), consistent with improved wound closure in the presence of 15LO1 inhibition (Fig. 4 *D*). Comparing the individual time points, BLX2477 improved wound closure at 16 hrs (n=6, p=0.042) and marginally at 8 hrs (n=6, p=0.090) (Fig. 4 *D*). There were no differences at other time points. There were no differences in starting wound area and DMSO alone did not alter the effect of IL-13 alone on wound closure (Fig. E6 in the Online Repository).

15LO1 inhibition increases Total Speed, but does not modify directionality as compared to IL-13

Movies E3 and E4 in the Online Repository demonstrate the complex cell movement patterns of DMSO and BLX2477/DMSO under IL-13 conditions, with Figures 5 *A, B* showing representative low and high magnification still images from 0-48 hrs, following wound closure. Matching phase-contrast images of the wound are shown in Figure E7 in the Online Repository.

Similar to total speed vs IL-13 treated cells, an FMM model was applied to compare Total and X-axis speed (Fig. 6 *A, B* and Table 2). By FMM, DMSO alone did not impact IL-13 induced migration (see Fig. E8, Table E6 and E7 in the Online Repository). In contrast, using FMM, the initial Total speed was higher in the IL-13+BLX group as compared to IL-13+DMSO, suggesting 15LO1 inhibition under IL-13 conditions increased the initial speed back towards that of untreated cells. Skewness was also significantly different between the two treatment groups, suggesting 15LO1 inhibition caused a more rapid decay in the original peak (Fig. 6 *A* and Table E8 in the Online Repository).

In contrast to IL-13 treated vs untreated, there were no differences in X-axis speed by FMM parameters between BLX2477 and DMSO treated cells (Fig. 6 *B*, and Table E9

in the Online Repository).

As FMM supported differences in Total speed under 15LO1 inhibition conditions, differences in Total speed at individual 20 min time points were compared (Fig. 6 *C*). Although there was a significant difference in the speed at the initial time point between IL-13+BLX group compared to the IL-13+DMSO by paired t-test ($p = 0.0148$), consistent with the results reported by FMM; after adjusting for multiple testing this result was not significant. More generally, when adjusted for multiple testing, there were no differences in Total speed during any of the first 24 hr time points. In contrast, in the second 24 hr period, Total speed was significantly higher in the IL-13+BLX group compared to the IL-13+DMSO group at all 72 time points measured even when correcting for multiple comparisons (See Table E10 and E11 in the Online Repository).

Since there were no differences in FMM analysis of X-axis speed (Fig. 6 *D* and Table E9 in the Online Repository), Acceleration comparisons between IL-13+BLX vs IL-13+DMSO were also not significant after BH correction (See Fig. E9 and Table E14 in the Online Repository).

Journal Pre-proof

Discussion

The ability of surface cells, such as AECs, to rapidly heal wounds is critical for maintenance of an organ's barrier function and overall health[21–24]. Indeed, the human asthmatic epithelium is markedly abnormal, associated with increased goblet cell differentiation, loss of cilia, junction proteins and altered wound repair[2,14,15,21,25,26]. The studies presented here identify the negative overall impact of a mediator known to be critical to asthma, IL-13, on epithelial wound repair, while dissecting its specific impact on migration. These studies were done using a highly novel real-time/time-lapse confocal microscopic system to evaluate the speed, acceleration and direction of movement of individual IL-13 treated polarized asthmatic cells compared to untreated cells. The complex multi-directional migration patterns were analyzed using novel statistical analyses to broadly and specifically describe the profound impact of IL-13 on speed and direction of migration. Finally, the studies provide preliminary data to suggest that the ferroptosis related 15LO1 pathway contributes to some of these IL-13-driven effects.

Detailed evaluation of single epithelial cell migratory patterns has previously been reported in monolayer culture systems[7]. However, evaluation of wound healing and associated migratory patterns of epithelial cells under the polarized conditions which most closely mimic *in vivo* airway conditions, has remained problematic. Cells form an intact plane and borders are difficult to identify[15]. In addition, time-lapse evaluation requires that the cells remain under the microscope objective, in an ALI state, for up to 48 hrs. Finally, these multilayered systems have been difficult to evenly wound using a manual scrape system, often leading to considerable tearing and folding of the epithelial systems. Our approach began by utilizing a novel, semi-automated device to consistently and reproducibly "wound" these complex epithelial cultures. Using nuclear identification, we then located the precise position of AECs under ALI conditions and

tracked the migration of single cells over 48 hrs.

Modeling nonlinear patterns for complex biological systems is a nontrivial problem. This is particularly true of modeling the temporal migratory patterns of cells considered in this paper. The FMM model is a parsimonious parametric model that was originally devised for describing rhythmic data. However, as demonstrated in Rueda et al[20], the model is very flexible to describe nonlinear and nonrhythmic patterns.

Using more traditional approaches, we recently reported abnormally slow wound repair of polarized asthmatic as compared to healthy AECs[4]. This abnormal repair was linked to higher FeNO, a typical T2/IL-13 biomarker (*in vivo*). Yet, the underlying mechanisms, particularly in relation to T2 inflammation remained poorly understood[26,27]. To further address this, we utilized the novel wounding system described here to target the effect of IL-13 differentiation on the wound repair process. Not surprisingly, we observed a profound effect of IL-13 to delay repair of polarized asthmatic AECs over 48 hrs. We then employed real-time confocal imaging and FMM analyses to determine the impact of IL-13 on the astonishingly complex migratory patterns we observed (See Supplementary Movies in the Online Repository).

Under IL-13 conditions, the Total cellular speed was initially slower and never reached the migratory speeds of untreated cells. They more briefly accelerated and then rapidly plateaued and remained at a generally constant acceleration compared to 0 $\mu m/h^2$, while untreated cells dynamically accelerated and then decelerated over wide ranges. X-axis directionality of IL-13 treated cells was maintained for a longer period given the slower wound closure, but changes in X-axis speed/directionality were never as high as untreated cells. These measures all support a more “sluggish” overall nature of the IL-13 treated cell movement as compared to the considerably more dynamic

movement of untreated cells.

Our findings are generally consistent with those of Losifidis et al, who reported submerged/single layer AECs from wheezing young children migrated more slowly and with less directionality than AECs from non-wheezing children[2]. Based on lower expression levels identified *ex vivo*, these abnormalities were linked to lower activation of the phosphatidyl inositol 3 kinase (PI3K) pathway in the asthmatic cells, a pathway intimately tied to the IL-4 receptor alpha[28,29]. This slow migration observed in AECs from pre-asthmatic children, and now in adult asthmatic AECs treated with IL-13, is also consistent with abnormal jamming/unjamming, as proposed by Park et al, in which AECs from asthma participants have delayed jamming, potentially due to AEC shape changes and force interactions, but independent of epithelial-mesenchymal transition [30–32]. It is important to point out that all cells studied here were asthmatic cells, given their known baseline differences from healthy cells. No comparison to healthy cells was performed. Thus, the impact of IL-13 on these already abnormal asthmatic AECs could serve to only magnify the basal differences from healthy cells.

To expand on biologic mechanism, and based on our published work with 15LO1, we hypothesized that the enzyme 15LO1, highly induced by IL-13 in AECs, could be playing a role in this dysfunction. Our previous studies showed that 15LO1 pathway activity is critical for inducing goblet cell differentiation, as well as ferroptotic and autophagic processes in human AECs[10–13]. Activation of 15LO1 consumes large quantities of reduced glutathione to “metabolize” ferroptotic phospholipids, including 15 HpETE-PE. As a further defense against cell death, AECs stimulated with IL-13 activate autophagy, indicative of stressed cells[13]. To investigate the role of the 15LO1 pathway further, we employed the 15LO1 inhibitor, BLX2477, which specifically inhibits 15LO1 activity[11,12]. In fact, we observed small but significant improvements in

wound closure under IL-13 conditions in the presence of this inhibitor (Fig. 4). By FMM analysis, differences in Total speed and skewness were observed between the BLX2477 treated and DMSO treated cells, consistent with the improvement in Total speed by paired T-testing from 24-48 hrs.

Studies of wound repair in primary human asthmatic AECs are not without limitation. Each of our samples (total n=12) came from different individual MMA patients, to control for differences in wound repair between asthmatic and healthy cells. However, obtaining these cells requires bronchoscopy of consenting adults and nearly a month of culture time before studies can be performed. These rigorous requirements limit the numbers of samples available. However, the methodologies employed here allowed us to detect physiologic and biologic differences despite these small sample sizes. Comparison of healthy and asthmatic cells treated with IL-13 are also needed to determine whether the IL-13 effect occurs additively or synergistically with baseline differences between asthmatic and healthy AECs.

In conclusion, we report a novel wound repair system for polarized AECs which utilizes a highly innovative confocal microscopic approach combined with cutting-edge biostatistics to quantify the movement of individual cells. Using this methodology, we identified substantial abnormalities in the migration patterns of asthmatic AECs additionally treated with IL-13 compared to untreated cells. These factors contributed to markedly slower wound closure of IL-13 treated cells, which was modestly reversed by a 15LO1 inhibitor, suggesting its potential as an asthma therapeutic. The systems and approaches used here offer novel ways to dynamically monitor complex cell movements, even in multilayered systems over time and under wounded conditions.

Journal Pre-proof

Acknowledgements

This study was supported by 1 R01 AI145406-01A1, 1 R01 HL153058-01, 5 P01 AI106684-05; and donations from the Dellenback family. We thank Hans-Erik Claesson for providing BLX2477. We also thank Travis Wheeler at the University of Pittsburgh machine shop for making the wounding device.

Author contributions

M.J. designed and carried out most of the experiments and drafted the manuscript. S.W. designed the confocal migration system. Y.G.L. and S.P. developed, designed and performed FMM analysis for migration speed and direction. C.W. and C.S.C. maintained the live-cell microscopy system and designed the computer analyses of migration data. X.Z. assisted with sample preparation, wounding and western blot. J.Z. assisted with sample preparation, wounding and western blot and helped to design elements of the wound repair and migration experiments. S.E.W. conceived the study, assisted with design elements and analysis, and wrote and edited the manuscript.

Journal Pre-proof

References

1. Masoli M, Fabian D, Holt S, Beasley R. The global burden of asthma: executive summary of the GINA Dissemination Committee Report. Allergy. 2004;59:469–78.

2. Iosifidis T, Sutanto EN, Buckley AG, Coleman L, Gill EE, Lee AH, et al. Aberrant cell migration contributes to defective airway epithelial repair in childhood wheeze. JCI Insight [Internet]. 2020 [cited 2020 Jun 5];5. Available from: https://insight.jci.org/articles/view/133125

3. Moffatt MF, Phil D, Gut IG, Strachan DP. A Large-Scale, Consortium-Based Genomewide Association Study of Asthma. The New England Journal of Medicine. 2010;11.

4. Inoue H, Hattori T, Zhou X, Etling EB, Modena BD, Trudeau JB, et al. Dysfunctional ErbB2, an EGF receptor family member, hinders repair of airway epithelial cells from asthmatic patients. Journal of Allergy and Clinical Immunology. 2019;143:2075-2085.e10.

5. Nicodemus-Johnson J, Myers RA, Sakabe NJ, Sobreira DR, Hogarth DK, Naureckas ET, et al. DNA methylation in lung cells is associated with asthma endotypes and genetic risk. JCI Insight [Internet]. 2016 [cited 2021 Jan 6];1. Available from: https://insight.jci.org/articles/view/90151

6. Modena BD, Bleecker ER, Busse WW, Erzurum SC, Gaston BM, Jarjour NN, et al. Gene Expression Correlated with Severe Asthma Characteristics Reveals Heterogeneous Mechanisms of Severe Disease. Am J Respir Crit Care Med. 2017;195:1449–63.

7. Lee S-N, Ahn J-S, Lee SG, Lee H-S, Choi AMK, Yoon J-H. Integrins αvβ5 and αvβ6 Mediate IL-4–induced Collective Migration in Human Airway Epithelial Cells. Am J Respir Cell Mol Biol. 2018;60:420–33.

8. Ahdieh M, Vandenbos T, Youakim A. Lung epithelial barrier function and wound healing are decreased by IL-4 and IL-13 and enhanced by IFN-γ. American Journal of Physiology-Cell Physiology. 2001;281:C2029–38.

9. Chu HW, Balzar S, Westcott JY, Trudeau JB, Sun Y, Conrad DJ, et al. Expression and activation of 15-lipoxygenase pathway in severe asthma: relationship to eosinophilic phenotype and collagen deposition. Clin Exp Allergy. 2002;32:1558–65.

10. Zhao J, Maskrey B, Balzar S, Chibana K, Mustovich A, Hu H, et al. Interleukin-13-induced MUC5AC is regulated by 15-lipoxygenase 1 pathway in human bronchial epithelial cells. Am J Respir Crit Care Med. 2009;179:782–90.

11. Zhao J, O'Donnell VB, Balzar S, Croix CMS, Trudeau JB, Wenzel SE. 15-Lipoxygenase 1 interacts with phosphatidylethanolamine-binding protein to regulate MAPK signaling in human airway epithelial cells. PNAS. 2011;108:14246–51.

12. Wenzel SE, Tyurina YY, Zhao J, St. Croix CM, Dar HH, Mao G, et al. PEBP1 Wardens Ferroptosis by Enabling Lipoxygenase Generation of Lipid Death Signals. Cell. 2017;171:628-641.e26.

13. Zhao J, Dar HH, Deng Y, St. Croix CM, Li Z, Minami Y, et al. PEBP1 acts as a rheostat between prosurvival autophagy and ferroptotic death in asthmatic epithelial cells. Proc Natl Acad Sci USA. 2020;201921618.

14. Iosifidis T, Garratt LW, Coombe DR, Knight DA, Stick SM, Kicic A. Airway epithelial repair in health and disease: Orchestrator or simply a player? 2016;11.

15. Looi K, Buckley AG, Rigby PJ, Garratt LW, Iosifidis T, Zosky GR, et al. Effects of human rhinovirus on epithelial barrier integrity and function in children with asthma. Clinical & Experimental Allergy. 2018;48:513–24.

16. Amatngalim GD, Broekman W, Daniel NM, van der Vlugt LEPM, van Schadewijk A, Taube C, et al. Cigarette Smoke Modulates Repair and Innate Immunity following Injury to Airway Epithelial Cells. PLoS One. 2016;11:e0166255.

17. van Riet S, Ninaber DK, Mikkers HMM, Tetley TD, Jost CR, Mulder AA, et al. In vitro modelling of alveolar repair at the air-liquid interface using alveolar epithelial cells derived from human induced pluripotent stem cells. Sci Rep. 2020;10:5499.

18. Chu HW, Balzar S, Seedorf GJ, Westcott JY, Trudeau JB, Silkoff P, et al. Transforming Growth Factor-β2 Induces Bronchial Epithelial Mucin Expression in Asthma. The American Journal of Pathology. 2004;165:1097–106.

19. Zhao J, Minami Y, Etling E, Coleman JM, Lauder SN, Tyrrell V, et al. Preferential Generation of 15-HETE-PE Induced by IL-13 Regulates Goblet Cell Differentiation in Human Airway Epithelial Cells. Am J Respir Cell Mol Biol. 2017;57:692–701.

20. Rueda C, Larriba Y, Peddada SD. Frequency Modulated Möbius Model Accurately Predicts Rhythmic Signals in Biological and Physical Sciences. Sci Rep. 2019;9:18701.

21. Xiao C, Puddicombe SM, Field S, Haywood J, Broughton-Head V, Puxeddu I, et al. Defective epithelial barrier function in asthma. Journal of Allergy and Clinical Immunology. 2011;128:549-556.e12.

22. Stevens PT, Kicic A, Sutanto EN, Knight DA, Stick SM. Dysregulated repair in asthmatic paediatric airway epithelial cells: the role of plasminogen activator inhibitor-1. Clinical & Experimental Allergy. 2008;38:1901–10.

23. Kicic A, Hallstrand TS, Sutanto EN, Stevens PT, Kobor MS, Taplin C, et al. Decreased Fibronectin Production Significantly Contributes to Dysregulated Repair of Asthmatic Epithelium. Am J Respir Crit Care Med. 2010;181:889–98.

24. Lloyd CM, Snelgrove RJ. Type 2 immunity: Expanding our view. Science Immunology [Internet]. 2018 [cited 2020 Mar 14];3. Available from: https://immunology.sciencemag.org/content/3/25/eaat1604

25. Heijink IH, Kuchibhotla VNS, Roffel MP, Maes T, Knight DA, Sayers I, et al. Epithelial cell dysfunction, a major driver of asthma development. Allergy. 2020;75:1898–913.

26. Lambrecht BN, Hammad H. The airway epithelium in asthma. Nature Medicine. 2012;18:684–92.

27. Kubo M. Innate and adaptive type 2 immunity in lung allergic inflammation. Immunological Reviews. 2017;278:162–72.

28. Kelly-Welch AE. Interleukin-4 and Interleukin-13 Signaling Connections Maps. Science. 2003;300:1527–8.

29. Harb H, Chatila T. Mechanisms of Dupilumab. Clin Exp Allergy. 2020;50:5–14.

30. Mitchel JA, Das A, O'Sullivan MJ, Stancil IT, DeCamp SJ, Koehler S, et al. In primary airway epithelial cells, the unjamming transition is distinct from the epithelial-to-mesenchymal transition. Nature Communications. 2020;11:5053.

31. Park J-A, Kim JH, Bi D, Mitchel JA, Qazvini NT, Tantisira K, et al. Unjamming and cell shape in the asthmatic airway epithelium. Nat Mater. 2015;14:1040–8.

32. Park J-A, Fredberg JJ. Cell Jamming in the Airway Epithelium. 2016;13:4.

Journal Pre-proof

Figure Legends

FIG 1. IL-13 stimulation decreases wound closure compared to untreated cells. 2mm×10mm images were compared between untreated and IL-13 treated AECs. **A**, Representative images (10X objective) of IL-13 (10ng/ml) treated or untreated ALI cells. **B**, Higher magnification images from (A). **C**, IL-13 stimulation decreased overall wound closure compared to untreated cells by paired-AUC testing (p=0.028, n=6). At both 8 and 16 hrs, the area of the wound under IL-13 conditions was larger than that of the untreated cells (p=0.017, p=0.017 separately, n=6). There were no statistical differences at other time points.

FIG 2. AEC migration speed and patterns are altered by IL-13 as compared to untreated cells. **A**, AEC migration was tracked from the same culture regions as shown in Figure E4 in the Online Repository. Nuclei were automatically detected using IMARIS software. Colored lines represent the migration paths of AEC nuclei over the previous 3 hrs. Colors of lines identify specific time intervals after wounding. Blue represents 5-8 hrs; Light blue represents 13-16 hrs; Green represents 21-24 hrs; Light green represents 29-32 hrs; Yellow represents 37-40 hrs; Red represents 45-48 hrs. **B**, Higher magnification migration images (3 times magnified, 0.7mm×0.7mm) of (A).

FIG 3. Statistical analyses identify specific differences in the complex migratory patterns of IL-13 stimulated AECs after wounding as compared to untreated cells. (See also Tables 1 and 2). **A**, FMM for Total speed of untreated vs IL-13 treated AECs. The fitted FMM curve for untreated AECs is shown as the solid blue line. The fitted FMM curve for IL-13 treated AECs is shown as the solid red line. **B**, FMM for X-axis speed of untreated vs IL-13 treated AECs. The fitted FMM curve for untreated AECs is shown as the solid blue line. The fitted FMM curve for IL-13 treated AECs is shown as the solid red line. **C**, Total migratory speed (mean with SEM scale bars) **D**, X-axis migratory speed [net speed toward wound (mean with SEM scale bars)]. **E**, Acceleration curves for untreated and IL-13 treated AECs in 24 hrs. The acceleration of IL-13 treated AECs rapidly decreased to ~0 $\mu m/h^2$ by 6 hrs, whereas untreated AECs maintained acceleration until 9 hrs before decelerating. After 12 hrs, untreated AECs decelerated rapidly at first and then went back from lowest negative value at 15 hrs to ~0 $\mu m/h^2$ at 21-24 hrs. IL-13 treated AECs continued decelerating even after 12 hrs. Statistically significant differences are shown on the figure, where the acceleration is higher or lower than 0 $\mu m/h^2$.

FIG 4. Chemical inhibition of 15LO1 under IL-13 conditions improves wound closure compared to IL-13 alone. **A**, Confirmation of 15LO1 protein increases by IL-13 in ALI-cultured AECs. **B**, Representative images (10× objective) of wound closure between IL-13+DMSO vs IL-13+BLX treated AECs. **C**, Magnified 2mm×2mm images of those in (B). **D**, 15LO1 inhibition with BLX2477 improved wound closure as compared to IL-13+DMSO AECs by paired-AUC testing (p=0.034, n=6). At 16 hrs, the area of the wound was smaller under IL-13+BLX treated conditions, as compared to IL-13+DMSO conditions was larger than that of the untreated cells (p=0.042, n=6). There were no statistical differences at other time points.

FIG 5. 15LO1 inhibition marginally improves AEC migratory patterns under IL-13 conditions towards that of IL-13+DMSO AECs. **A**, AECs migration was tracked from the same culture regions as those shown in Figure E7 in the Online Repository. Nuclei were automatically detected using IMARIS software. Colored lines represent the migration paths of AEC nuclei over the previous 3 hrs. Colors of lines identify specific time intervals after wounding. Blue represents 5-8 hrs; Light blue represents 13-16 hrs; Green represents 21-24 hrs; Light green represents 29-32 hrs; Yellow represents 37-40 hrs; Red represents 45-48 hrs. **B**, Higher magnification migration images (3 times magnified, 0.7mm×0.7mm) of (A).

FIG 6. Statistical analyses identify specific differences in the complex migratory patterns

of IL-13 stimulated AECs after wounding as compared to IL-13 stimulated cells in the presence of 15LO1 inhibition (See also Tables E8 and E9 in the Online Repository). **A**, FMM for Total speed of IL-13+BLX vs IL-13+DMSO treated AECs. The fitted FMM curve for IL-13+BLX treated AECs is shown as the solid green line. The fitted FMM curve for IL-13+DMSO treated AECs is shown as the solid brown line. **B**, FMM for X-axis speed of IL-13+BLX vs IL-13+DMSO treated AECs. The fitted FMM curve for IL-13+BLX treated AECs is shown as the solid green line. The fitted FMM curve for IL-13+DMSO treated AECs is shown as the solid brown line. **C**, Total migratory speed (mean with SEM scale bars). **D**, X-axis migratory speed [net speed toward wound (mean with SEM scale bars)]

Journal Pre-proof

635 **Tables**

Table 1. FMM analysis of Total speed (Untreated vs IL-13 treated AECs) with the different components

	Untreated	IL13	Difference
FMM parameters	Estimate (SE)	Estimate (SE)	Difference (95%CI)
Initial speed	35.06 (9.43)	14.63 (2.94)	20.43 (11.45,29.42)*
Amplitude	11.66 (3.76)	12.98 (5.58)	-1.31 (-8.21,5.58)
Skewness	-0.04 (0.67)	0.01 (0.54)	-0.04 (-0.82,0.74)
Peakedness	0.26 (0.13)	0.33 (0.12)	-0.07 (-0.24,0.09)
Peak Time (hours)	10.16 (0.97)	6.0 (0.75)	4.16 (3.04,5.27)*

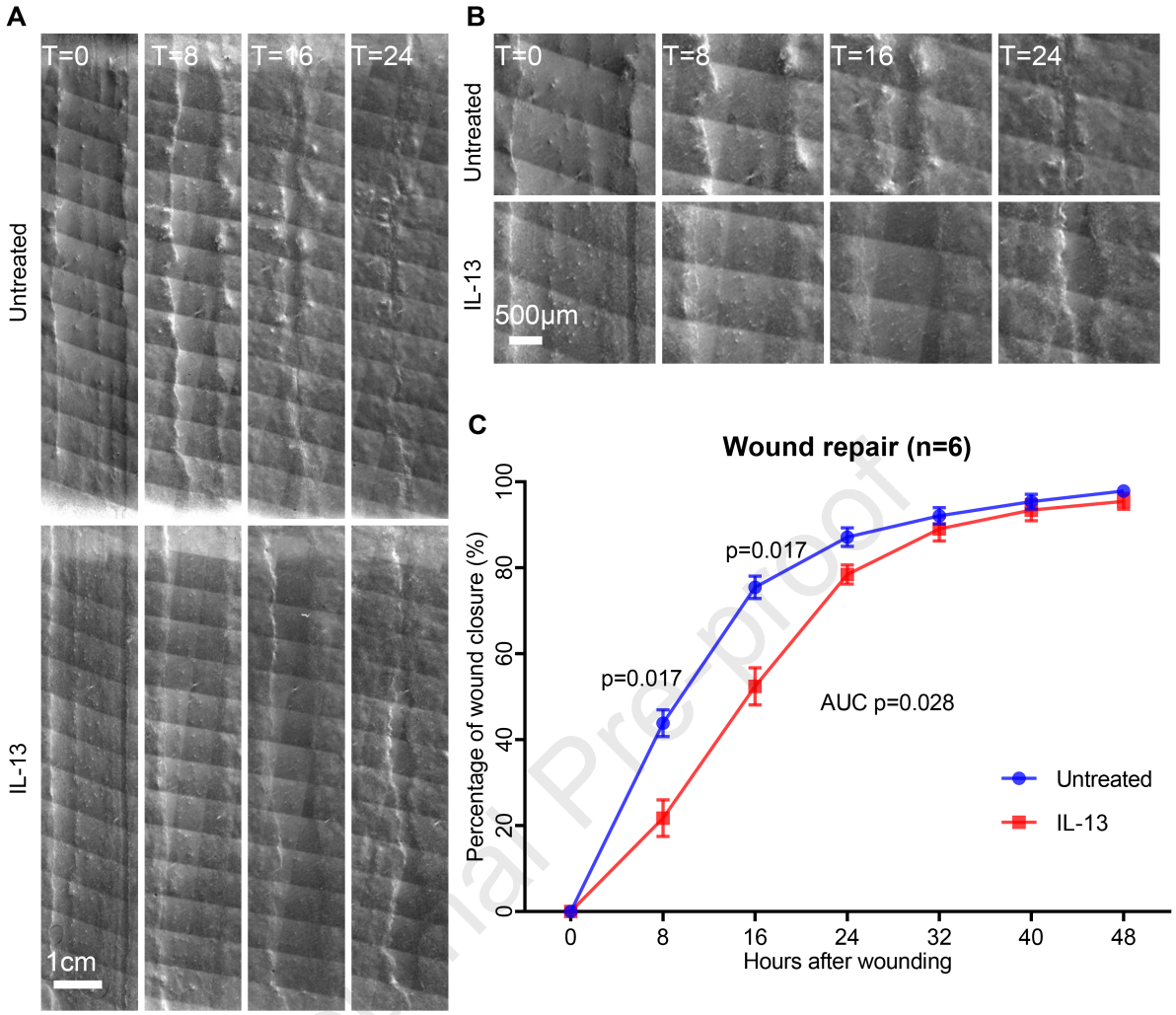
636 Significant p-values are labeled with asterisk *, P < 0.05.
637

Table 2. FMM analysis of X-axis speed (Untreated vs IL-13 treated AECs) with the different components

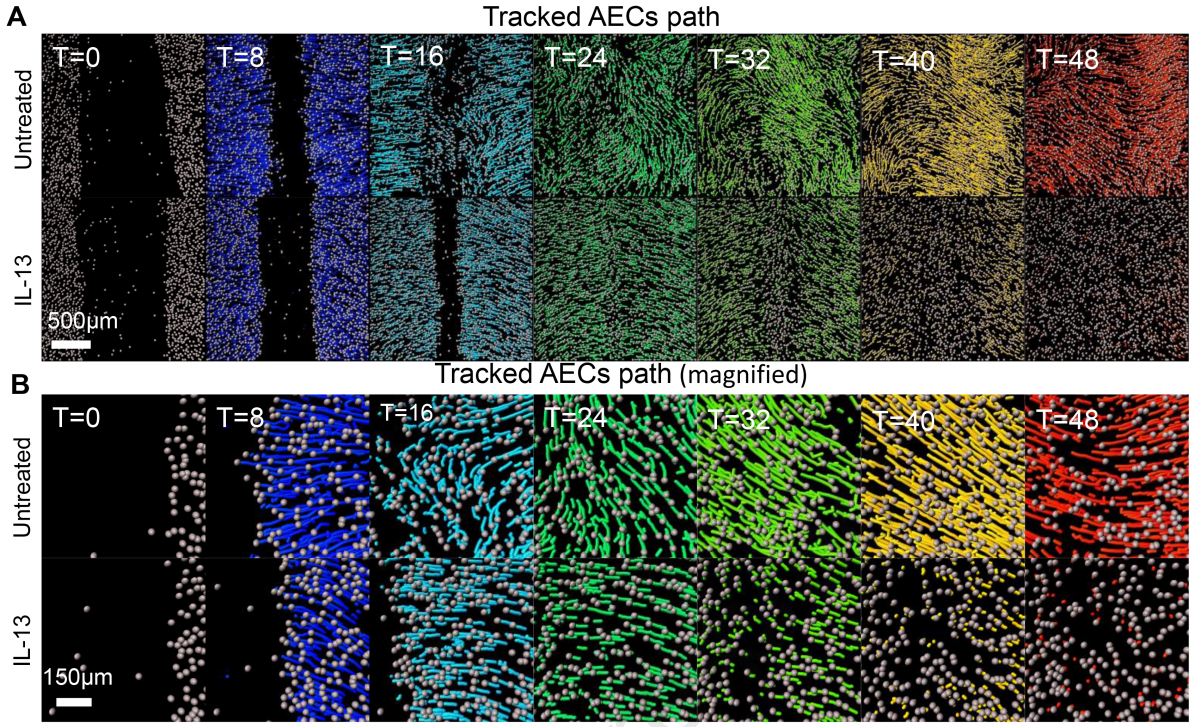
	Untreated group	IL13 group	Difference
FMM parameters	Estimate (SE)	Estimate (SE)	Difference (95%CI)
Initial speed	8.31 (4.61)	8.99 (3.45)	-0.68 (-5.92,4.56)
Amplitude	24.83 (3.87)	13.34 (7.38)	11.49 (3.92,19.07)*
Skewness	-0.81 (0.21)	0.09 (0.58)	-0.89 (-1.45,-0.34)*
Peakedness	0.47 (0.12)	0.36 (0.15)	0.11 (-0.06,0.28)
Peak Time (hours)	8.95 (0.87)	7.06 (0.87)	1.89 (0.77,3.02)*

638 Significant p-values are labeled with asterisk *, P < 0.05.
639

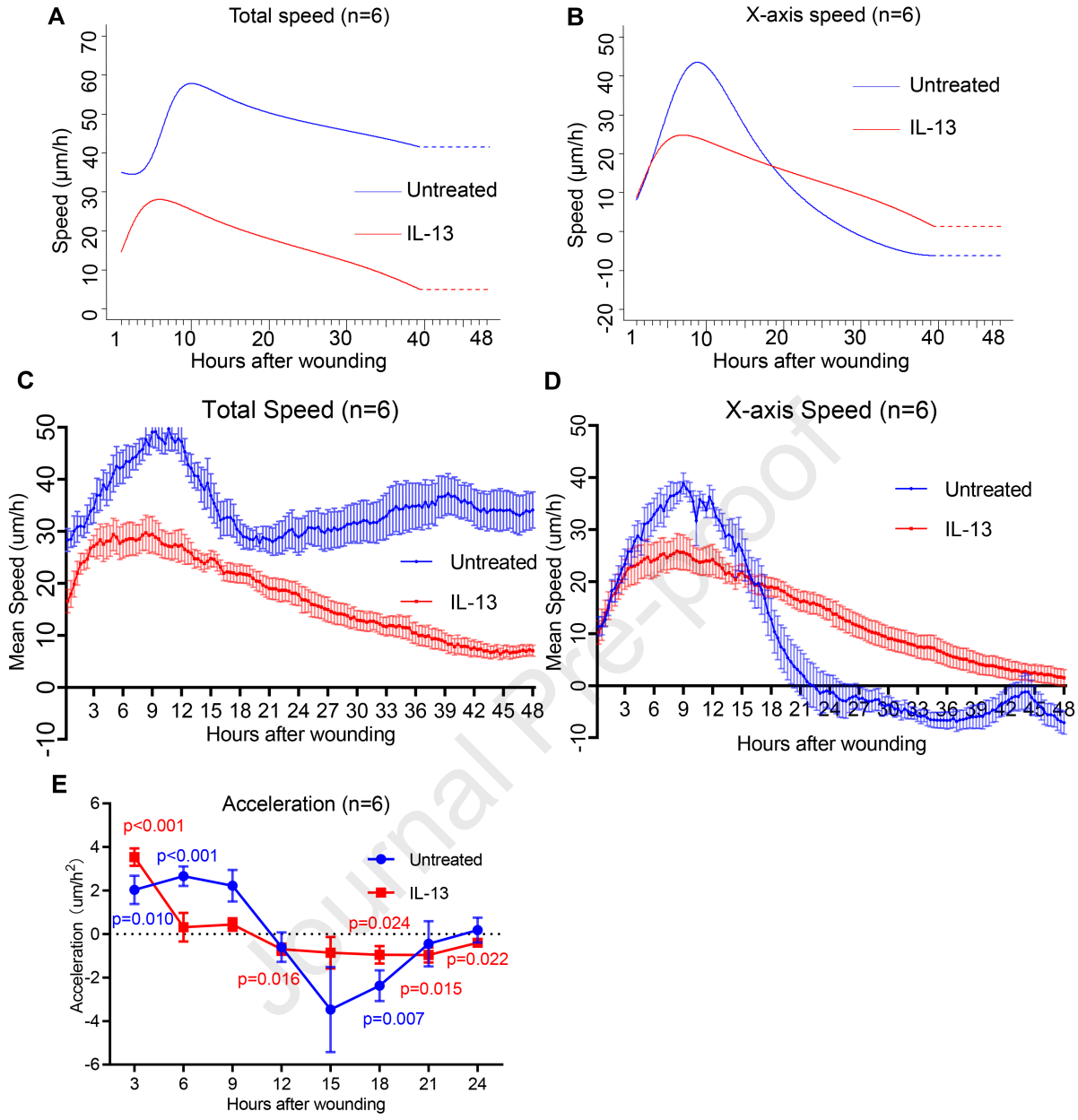
Journal Pre-proof



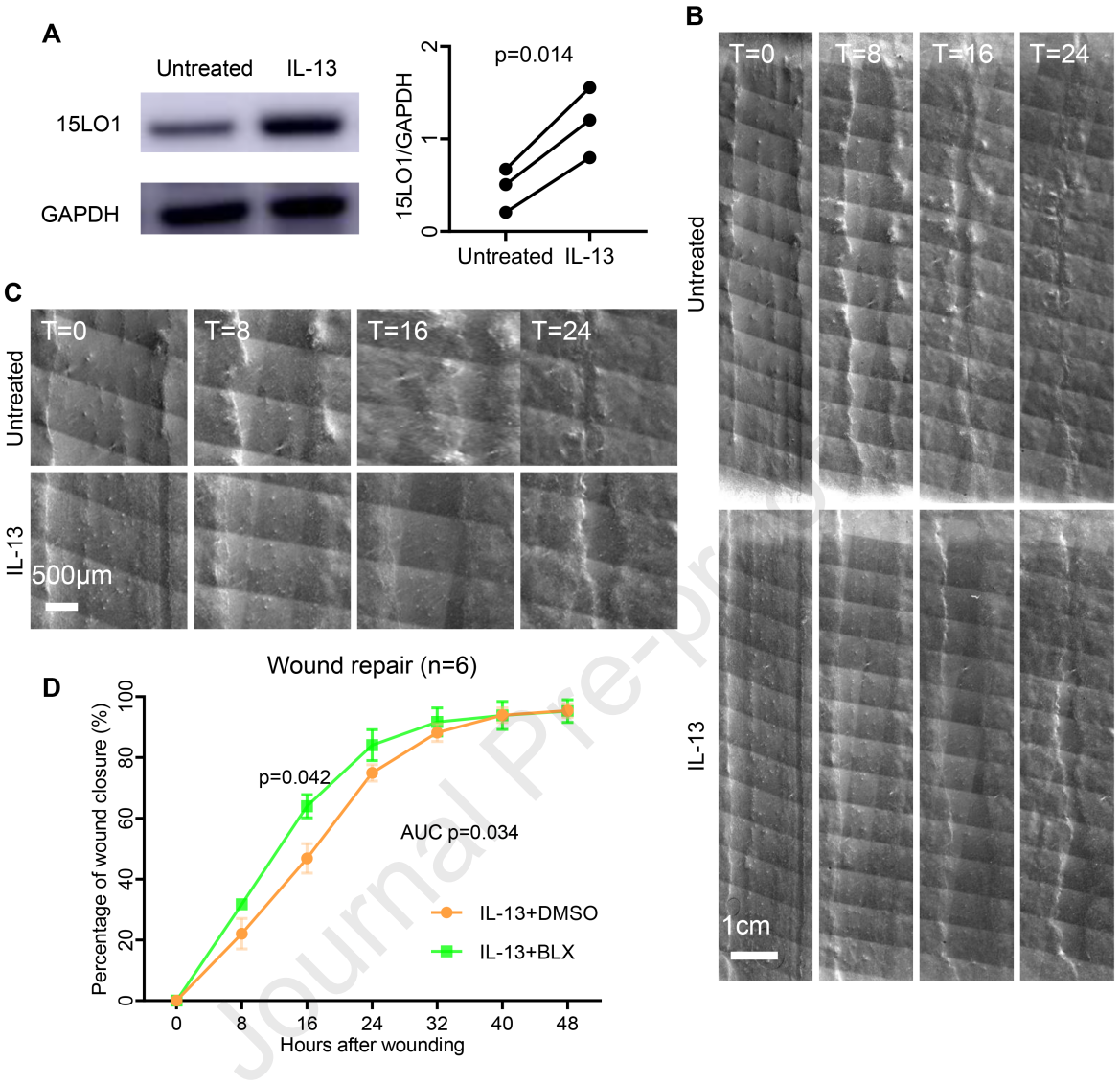
Journal Pre-proof



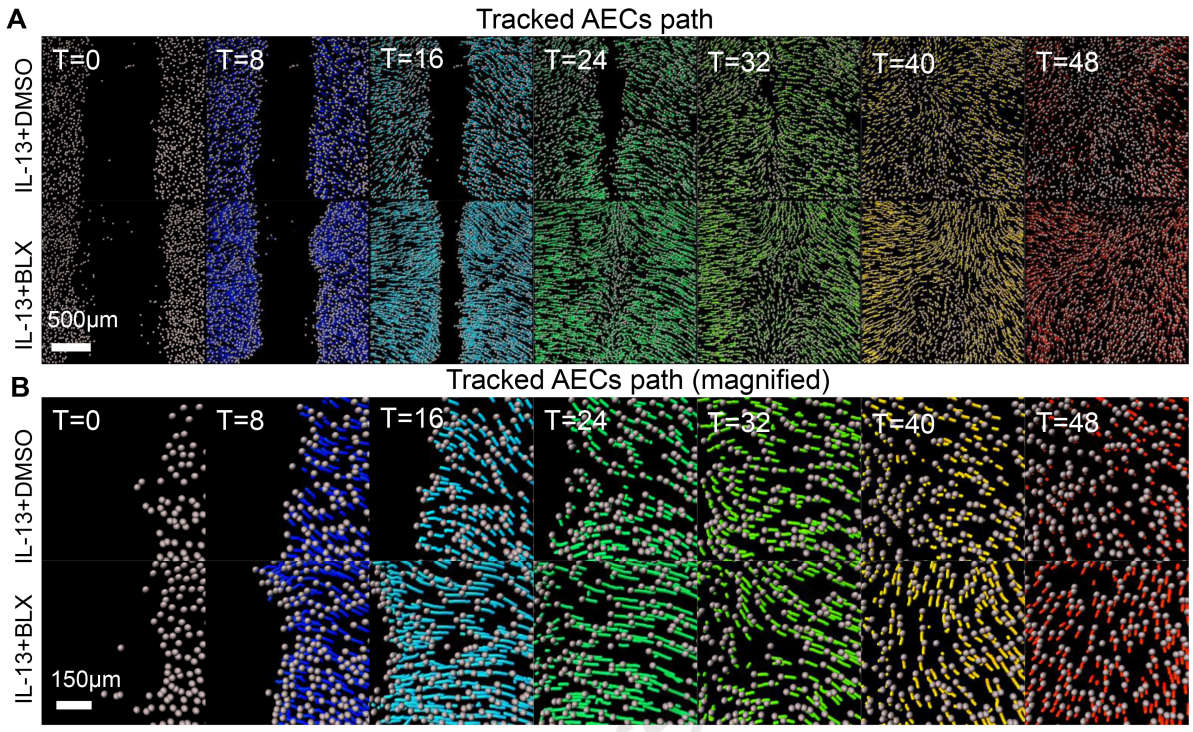
Journal Pre-proof



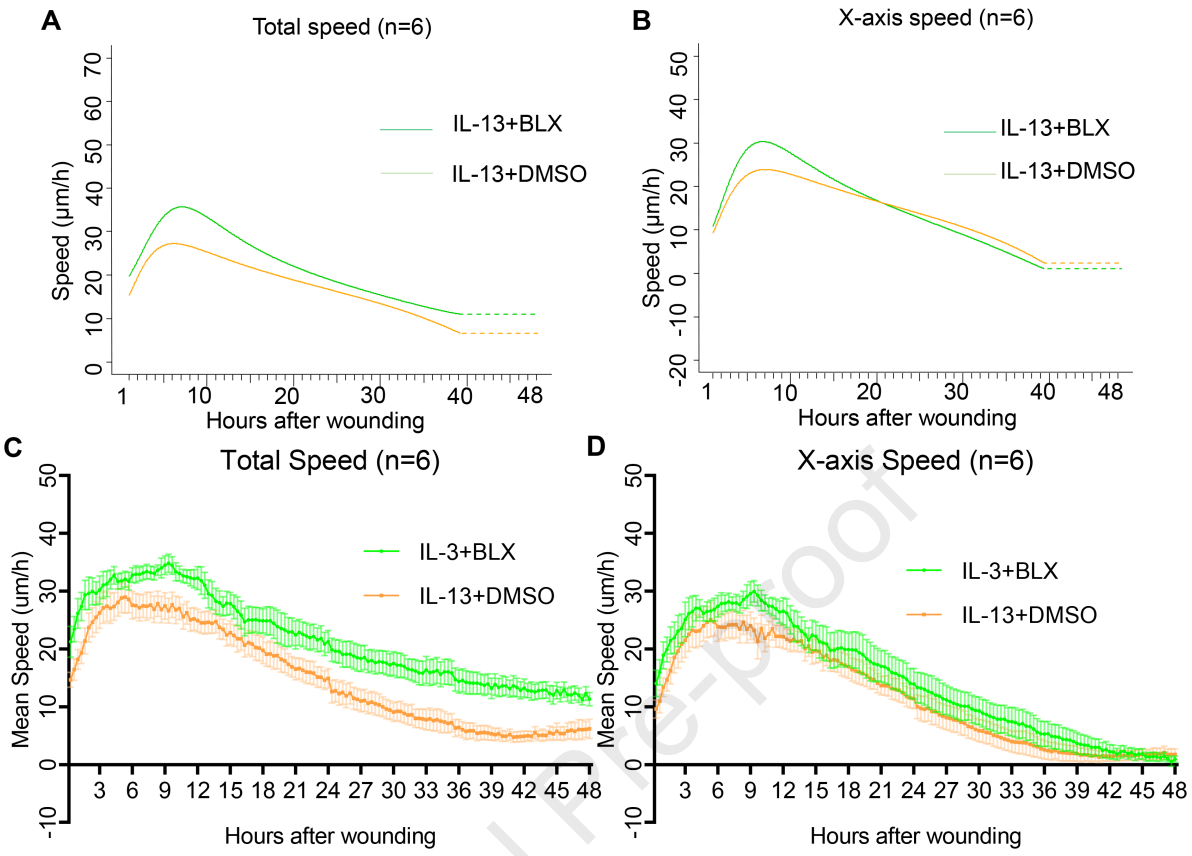
Journal Pre-proof



Journal Pre-proof



Journal Pre-proof



Journal Pre-proof